Three types of A11 neurons project to the rat spinal cord

Hidechika Ozawa[1]*, Tsuyoshi Yamaguchi[2]*, Shinsuke Hamaguchi[1], Shigeki Yamaguchi[1], Shuichi Ueda[2]

[1]Department of Anesthesia and Pain Medicine, Dokkyo Medical University School of Medicine, Tochigi, Japan

[2]Department of Histology and Neurobiology, Dokkyo Medical University School of Medicine, Tochigi, Japan

*These authors contributed equally to this work.

Correspondence to:

Shuichi Ueda, Department of Histology and Neurobiology, Dokkyo Medical University School of Medicine, 880 Kita-kobayashi, Mibu-machi, Shimotsuga-gun, Tochigi 321-0293, Japan

Phone: +81-282-87-2124

Fax: +81-282-86-1463

E-mail: shu-ueda@dokkyomed.ac.jp

Acknowledgments

This work was supported by Dokkyo Medical University. H.O. is the recipient of a Young Investigator award (No.2015-21) from Dokkyo Medical University. We would like to thank Shukuko Nihei for excellent technical assistance.

ABSTRACT

The A11 dopaminergic cell group is the only group among the A8–A16 dopaminergic cell groups that includes neurons innervating the spinal cord, and a decrease in dopaminergic transmission at the spinal cord is thought to contribute to the pathogenesis of restless legs syndrome. However, the mechanisms regulating the neuronal activity of A11 dopaminergic neurons remain to be elucidated. Unraveling the neuronal composition, distribution and connectivity of A11 neurons would provide insights into the mechanisms regulating the spinal dopaminergic system. To address this, we performed immunohistochemistry for calcium-binding proteins such as calbindin (Calb) and parvalbumin (PV), in combination with the retrograde tracer Fluorogold (FG) injected into the spinal cord.

Immunohistochemistry for Calb, PV, or tyrosine hydroxylase (TH), a marker for dopaminergic neurons, revealed that there were at least three types of neurons in the A11 region: neurons expressing Calb, TH, or both TH and Calb, whereas there were no PV-immunoreactive (IR) cell bodies. Both Calb- and PV-IR processes were found throughout the entire A11 region, extending in varied directions depending on the level relative to bregma. We found retrogradely labeled FG-positive neurons expressing TH, Calb, or both TH and Calb, as well as FG-positive neurons lacking both TH and Calb.

These findings indicate that the A11 region is composed of a variety of neurons that are distinct in their neurochemical properties, and suggest that the dienccephalospinal dopamine system may be regulated by both Calb-IR and PV-R processes within the A11 region, as well as by Calb-IR processes derived from the A11 region at the terminal region of the spinal cord.

Keywords: A11 region; heterogeneity; calbindin; tyrosine hydroxylase; restless legs syndrome

INTRODUCTION

Dopamine plays crucial roles in a variety of physiological functions such as reward, motor function, motivation, goal-directed behavior, memory, learning and pain [1-3]. Dopaminergic neurons are enriched in several brain regions designated as A8–A16 [1]. Among these, the A11 dopaminergic system is the only dopaminergic system that gives rise to descending projections to the spinal cord [2, 4-5]. In addition to these particular neural connections, the fact that dopaminergic receptors are present in the spinal cord, and that dopamine receptor agonists alleviate the symptoms of restless legs syndrome (RLS), led to the hypothesis that hypo-activity of A11 neurons is a contributing factor in the pathogenesis of RLS [3]. However, the mechanisms regulating or modulating the A11 dopaminergic system remain to be elucidated.

Regarding the regulation or modulation of activity of the A11 dopaminergic system, electron microscopy revealed that dopaminergic neurons of the A11 region were innervated by inhibitory inputs of gamma-aminobutyric acid (GABAergic) terminals [6]. However, it is unknown whether the terminals of these GABAergic neurons are derived from neighboring neurons or from other brain entities outside the A11 region, or whether excitatory inputs innervate the dopaminergic neurons of the A11 dopaminergic system. Several recent lines of evidence have suggested functional heterogeneity of the A11 region, in which distinct components of the A11 region carry out distinct physiological functions. For example, Pappas et al. demonstrated that neurons in the caudal aspect of the A11 region have more responsibility for dopamine release at the spinal cord than those in the rostral aspect [7]. Abdallah et al. demonstrated that neurons in the rostral to middle aspect of the A11 region are more activated than those in the caudal part during migraine [8]. However, it is unknown whether the A11 region has heterogeneity in its morphological organization.

Many regions of the central nervous system have been found to display heterogeneity in neuronal composition using immunohistochemistry for calcium-binding proteins as distinctive markers for many neuronal populations [9]. These areas include the cortex, substantia nigra [10], ventral tegmental area [11], thalamus [12], striatum, nucleus accumbens [13-14], spinal cord and dorsal root ganglion [15]. In the A11 region, it was reported that almost all of the dopaminergic neurons (93% of TH-positive neurons) express calretinin and only a small population of dopaminergic neurons (9% of TH-positive neurons) express calbindin (Calb) [9]. To investigate the organization and neuronal composition of the A11 region, with emphasis on the distribution and connectivity of non-TH neurons, which may regulate or modulate the dopaminergic neurons, we performed immunohistochemistry for TH, Calb and PV.

MATERIALS AND METHODS

Animals

Adult male Sprague–Dawley (SD) rats (Charles River, Tsukuba, Japan) were housed under temperature- and humidity-controlled conditions on a 12-hour light/dark cycle with ad libitum access to food and water. All experiments were performed in accordance with the National Institutes of Health Guide for the Care and Use of Laboratory Animals and were approved by the Animal Research Committees of Dokkyo Medical University School of Medicine. All efforts were made to minimize animal suffering and the number of animals used in the study.

Fluorogold retrograde tracer injections

In five 8-week-old SD male rats, laminectomy was performed over the spinal cord region of interest. Unilateral injections of Fluorogold (FG; Fluorochrome, Englewood, CO) were placed between the L2 and L5 level of the spinal cord. FG (4%) was dissolved in 0.1 M sodium cacodylate and delivered using an iontophoresis pump (Kation Scientific, Minneapolis, MN) for 20 minutes with 7-s on/off intervals and positive pulses of 5 μA through a 1.0-mm glass pipette with a tip diameter of 50 μm. After the surgical procedure, the animals were maintained for 30 days before perfusion, to allow time for the neuronal tracer to be retrogradely transported.

Sample preparation for anatomical analysis

Four 8-week-old SD male rats were anesthetized with sodium pentobarbital (Kyoritsu Seiyaku, Tokyo, Japan) and transcardially perfused with 0.9% saline, followed by a fixative containing 4% paraformaldehyde in 0.1 M phosphate buffer (PB). Rat brains were removed and immersed in the fixative solution at 4°C overnight. The solution was replaced with 30% sucrose solution, and brains were frozen in dry ice powder. Sixteen-micrometer-thick coronal sections from rat brains were cut in a cryostat and collected sequentially in six receptacles containing 4% paraformaldehyde in 0.1 M PB. Sections were then put in a cryoprotectant solution containing 30% polyethylene glycol and 30% sucrose and stored at −20°C until use.

Immunohistochemistry

Consecutive sections were rinsed several times with 0.1 M phosphate-buffered saline (PBS) containing 0.3% Tween 20 (PBS-T). The free-floating sections were then put in a blocking solution containing 4% bovine serum albumin in PBS-T. After incubation in the blocking solution for 1 h, sections were put in a blocking solution with primary antibody directed against TH (1:500 dilution, Cat#AB152, Millipore, Darmstadt, Germany), Calb (1:500 dilution, Cat#C9848, Sigma-Aldrich, St. Louis, MO), PV (1:500 dilution, Cat#P3088, Sigma-Aldrich) or glutamate decarboxylase (GAD; 1:500, Cat#AB1511, Millipore) at 4°C overnight. The specificity of these primary antibodies was confirmed by comparison of

the immunostaining patterns with those of previous reports (Supplementary Information). Sections were then incubated for 2 h at room temperature in a 1:200 dilution of the fluorescence-conjugated secondary antibody (Alexa Fluor 568, Cat#A11036 for TH or GAD; Alexa Fluor 488, Cat#A11001 for Calb or PV, Invitrogen, Chicago, IL). After rinsing with PBS-T, sections were examined under a fluorescence microscope.

Data analysis

The histological material was examined with an AX80 microscope (Olympus, Tokyo, Japan) equipped with a DP-72 CCD camera (Olympus) and digital images were acquired using a BZ-X700 (Keyence, Tokyo, Japan) or BX-51 (Olympus) light microscope equipped with a DP-73 CCD camera (Olympus). All digital images were processed with Adobe Photoshop CC (Adobe Systems Inc., San Jose, CA). The nomenclature and boundaries of brain regions were determined using the Rat Brain Atlas [16].

Cell quantification

Acquired digital images were analyzed for cell quantification and cellular co-expression of TH, calbindin, or FG. A neuron was considered positive if immunoreactivity was at least 5 μm in diameter and observed in the entire cell body. A neuron was considered a double- or triple-labeled cell if the immunofluorescent pattern in one channel was identical to the other channel without changing focus.

Length measurement of a long axis in TH-IR neurons

A length of the long axis of a TH-IR cell within or outside the A11 region was measured using the measuring tool in the application software Adobe Photoshop CC.

RESULTS

Distribution of calbindin-immunoreactive cell bodies and processes within the A11 region

To determine whether Calb-IR neurons were present in the A11 region, we performed double-fluorescence immunohistochemistry for Calb and TH. The A11 region was readily identified on the basis of the presence of large cell bodies of TH neurons (arrows in Fig. 1). These A11 TH-IR neurons were distinguishable from small TH-IR neurons (arrowheads in Fig. 1c) belonging to other dopaminergic cell groups. We measured the long axis of TH-IR neurons within the A11 region, as well as those outside the A11 region. The average size of TH-IR neurons within the A11 region was 31.54 ± 0.9 μm (mean ± SEM, n = 78), and the average size of those outside of the A11 region was 15.66 ± 0.5 μm (mean ± SEM, n = 12). We also detected Calb-IR cell bodies throughout the entire rostro-caudal extent of the A11 region defined by the presence of large TH-IR neurons. These Calb-IR neurons were not distributed homogeneously within the A11 region and exhibited a gradient of distribution along the rostro-caudal axis (Fig. 1a'–1c').

At the rostral level (−3.24 mm from bregma), many intensely Calb-IR cell bodies were found scattered within the A11 region, as well as in the thalamus, which is dorsal to the mammillothalamic tract (mt), and the hypothalamus, which is ventral to the mt. At higher magnification (Fig. 2a–2a"), we found Calb-IR neurons intermingled with TH-IR neurons. Neurons co-expressing both TH and Calb as well as neurons expressing either TH (arrows) or Calb were detected (Fig. 3, Table). Among the cell bodies of these TH- and Calb-expressing neurons, Calb-IR long processes were found extending in a horizontal direction close to the cell bodies of TH-IR neurons (Fig. 2a").

At the middle level (−4.16 mm from bregma), we found a large number of intensely Calb-IR cell bodies within the A11 region. The density of Calb-IR cells was higher at this level than that at the rostral level. Those Calb-IR cell bodies were intermingled with those of TH-IR cells, which were located in the ventral aspect of the A11 region (Fig. 1b and 1b'). Similar to the rostral level, three types of cells, cells co-expressing both TH and Calb (double arrows), cells expressing TH and lacking Calb (arrows), and cells lacking TH and expressing Calb were observed at this level (Fig. 2b–2b", Fig. 3, and Table). We also observed more Calb-IR processes at this level than those at the rostral level, and these extended in various directions close to the TH-IR cell bodies.

At the caudal level (−4.44 mm from bregma), many Calb-IR cell bodies were observed. The density of the Calb-IR cell bodies was higher than that at the rostral level, and lower than that at the middle of the A11 region. We occasionally detected neurons expressing both Calb and TH as well as neurons expressing either TH or Calb (Fig. 2c–2c",).

Distribution of parvalbumin-immunoreactive cell bodies and processes within the A11 region

Parvalbumin (PV) is another calcium-binding protein, mainly expressed in fast-firing GABAergic neurons in many brain regions. To examine whether neurons expressing PV are present in the A11 region, we performed fluorescent immunolabeling for PV as well as double-fluorescent

immunolabeling for GAD and TH. There were a large number of intensely GAD-IR processes in the rostral and caudal aspects of the A11 region, and weaker GAD immunoreactivity was observed in the thalamus (upper region in Fig. 3a') and the middle aspect of the A11 region (Fig. 3b'). In contrast to the Calb immunoreactivity, PV-IR neuronal cell bodies were not detected, even though many PV-IR processes were detected throughout the A11 region (Fig. 3). The length and direction of these PV-IR processes varied depending on the distance from bregma.

At the rostral level (−3.24 mm from bregma), many PV-IR processes were observed among TH-IR cell bodies (arrows in Fig. 3d–3d"). These PV-IR processes were visible in the coronal sections as short processes extending in various directions, and appeared to be transverse sections of PV-IR processes extending in the rostral-caudal direction.

At the middle level (−4.16 mm from bregma), many PV-IR processes were observed as we observed at the rostral level (Fig. 3d'). In contrast to the PV-IR processes observed at the rostral level, we observed many long processes extending in the ventral-dorsal direction.

At the caudal level (−4.44 mm from bregma), we also observed many processes within the A11 region. Similar to the middle level of the A11, these processes were long processes in the coronal sections, extending in the ventral-dorsal direction (Fig. 3f').

Retrograde tracer Fluorogold injected in the rat spinal cord

We detected many retrogradely labeled FG-positive neurons within the A11 region of rats maintained for 1 month after FG injection into the spinal cord. Several types of FG-positive neurons were detected, including FG-positive neurons co-expressing both TH and Calb (double arrows in 5b–5bb"), and those expressing TH but not expressing Calb (arrows in Fig. 5b–5bb"). There were also FG-positive non-TH neurons expressing Calb (arrowheads in Fig. 5c–5cc") and lacking Calb (double arrowheads in Fig. 5c–5cc") within the A11 region. In addition to these FG-positive cells, we detected a few TH neurons that were not labeled by FG (open triangles in 5d–5dd").

DISCUSSION

In this study we demonstrated that the A11 region consists of a variety of neurons that are distinct in their neurochemical properties, using antibodies to TH and calcium-binding proteins. We observed that Calb-IR cell bodies of A11 neurons were intermingled with TH-IR cell bodies, and that Calb-IR cell bodies exhibited a characteristic distribution throughout the entire A11 region with processes extending among TH-IR neurons. In contrast to the profile of immunoreactivity for Calb, we did not detect any PV-IR cell bodies in this region even though we observed many PV-IR processes. Retrograde tracer experiments revealed that a variety of FG-positive neurons, including TH neurons either expressing or lacking Calb as well as non-TH neurons, projected to the rat spinal cord.

Neuronal heterogeneity within the A11 region

A growing body of evidence has been accumulating, showing that dopaminergic cell groups including A8–A10 consist of not only dopaminergic neurons but also a variety of neurons distinct in their neurochemical properties [11, 13-14, 17-26]. However, it is unclear whether the A11 region is similar to other dopaminergic cell groups in the heterogeneity of its neuronal composition. We demonstrated that there were subpopulations of TH-positive neurons; some co-expressed Calb and some did not express Calb. In addition to these TH-positive neurons, the A11 region also contained non-TH neurons expressing Calb and non-TH neurons lacking Calb. These results demonstrated that the A11 region is also heterogeneous in neuronal composition, similar to other dopaminergic cell groups.

Calbindin-immunoreactive cell bodies

It has long been known that there are two subpopulations of dopaminergic neurons in the midbrain with respect to expression of Calb (TH neurons expressing Calb and TH neurons lacking Calb), and that these subpopulations are distinct in their connectivity and physiological properties [10, 13-14, 27]. For instance, midbrain dopaminergic neurons expressing Calb preferentially project to the matrix of the striatum and are invulnerable to neurodegeneration [13-14]. Conversely, dopaminergic neurons lacking Calb preferentially project to the patches of the striatum and are vulnerable to neurodegeneration [13-14]. Our finding that some TH neurons express Calb may indicate that there are two subpopulations of TH neurons, distinct in their connectivity and/or physiological properties, within the A11 region.

In many brain regions, Calb-expressing neurons play a modulatory role. Calb-expressing neurons of the pedunculopontine nucleus include three types of neurons: glutamatergic, GABAergic, and cholinergic neurons. These neurons innervate the ventral tegmental area (VTA) and modulate the activity of dopaminergic neurons of the VTA [28-29]. In the medial thalamus such as the reuniens nucleus and ventromedial nucleus, half of the Calb-IR cells are co-localized with an excitatory neurotransmitter, aspartate or glutamate [30]. We demonstrated that Calb-IR cell bodies are present close to the TH-IR cell bodies, and many Calb-IR processes were extending among TH-IR cell bodies in the A11 region. Taken

together, our findings indicate that these Calb-IR neurons regulate activity of TH-IR neurons in the A11 region, although we were unable to exclude the possibility that these Calb-IR processes were derived from outside of the A11 region.

Parvalbumin-immunoreactive fibers

Electron microscopy has revealed that A11 dopaminergic neurons, as well as other hypothalamic dopaminergic neurons, are innervated by GABAergic terminals [6]. GABAergic neurons are classified into several groups on the basis of their neurochemical properties and one subpopulation of GABAergic neurons express PV [31]. However, the origin of these GABAergic neurons has not yet been identified. In the present study, we observed intensely GAD-IR processes within the A11 region as well as in the hypothalamus, and we only detected weakly PV-IR processes in A11, even though there were intensely PV-IR processes in the surrounding area. These results indicate that A11 dopaminergic neurons are mainly regulated or modulated by a PV-lacking subgroup of GABAergic neurons. In addition, we did not detect any PV-IR cell bodies within the A11 region, in spite of several reports demonstrating that GABAergic neurons are present in this region [8, 32-33]. Taken together, these results may indicate that non-PV-IR GABAergic neurons within or outside the A11 region regulate the activity of dopaminergic neurons of the A11 region.

Regional heterogeneity of the A11 region

Several lines of evidence have suggested that the A11 region exhibits functional heterogeneity. For instance, GABAergic neurons in the rostral to middle aspect of the A11 region are activated when facial nociceptive stimulation is applied [8]. TH neurons of the caudal A11 region are more responsible for dopamine release at the rat spinal cord than those of the rostral A11 region [7]. Our study revealed that coronal sections from the rostral levels of the A11 region contained short PV-IR processes that varied in direction, while the caudal levels of the A11 region contained long PV-IR processes in the perpendicular direction, indicating that processes observed in the rostral aspects of A11 were extending in the rostro-caudal direction and processes observed in the caudal aspects were extending in the ventral-dorsal direction. These results indicate that the A11 region exhibits morphological heterogeneity along the rostral-caudal axis. Part of the functional heterogeneity could be attributed to the differential morphological properties between the rostral and caudal A11 region.

Functional significance

Hypoactivity of A11 dopaminergic neurons is considered to be a contributing factor of restless legs syndrome. However, it is largely unknown how A11 dopaminergic neurons are regulated. Several reports have suggested a mechanism that regulates A11 dopaminergic neurons. Electron microscopy revealed that GABAergic terminals create a synapse on A11 dopaminergic neurons (van den Pol, 1986) and Pappas et al. demonstrated that opioid administration increases the

amount of dopamine release in the spinal cord, suggesting that A11 dopaminergic activity is activated via a 'dis-inhibitory' mechanism, which could be inhibition of GABAergic inputs (Pappas et al., 2011). However, the origin of these GABAergic inputs to A11 dopaminergic neurons remain to be shown. We demonstrated that the A11 region consists of not only dopaminergic neurons, but also non-TH neurons surrounding A11 TH neurons.

Although further investigation is needed to determine the neurochemical nature of these non-TH neurons, and whether these non-TH neurons electrophysiologically regulate neighboring TH neurons, our results demonstrate the possibility that A11 dopaminergic neurons are locally regulated.

Projection to the spinal cord

Dopaminergic (TH-positive) projections from the A11 region to the spinal cord have been reported previously [2, 4-5, 33]. In these previous studies, it was also reported that there were projections to the spinal cord derived from both non-TH and TH neurons of the A11 region. However, the neurochemical nature of the non-TH neurons remains to be elucidated. Some reports demonstrated that these non-TH neurons are GABAergic neurons by immunohistochemistry for GAD 65/67 [33], but Kosaka et al. reported that it is hard to detect GABAergic neurons of the A11 region by immunohistochemistry for GAD without colchicine treatment [32]. It is likely that only a small population of intensely GAD-positive neurons projecting to the spinal cord were detected by immunohistochemistry for GAD. In the present study, we demonstrated that several types of A11 neurons, including TH neurons, TH neurons co-expressing Calb, non-TH neurons expressing Calb and non-TH neurons lacking Calb, all project to the rat spinal cord. Although further investigations are needed to determine whether these non-TH neurons are excitatory or inhibitory, our results indicate that the descending pain inhibitory system via dopaminergic neurons is regulated by a variety of neurons with distinct neurochemical properties, both within the terminal region of the A11 neurons at the spinal cord and locally within the A11 region.

Funding:

This study was funded by a Young Investigator Award (grant number 2015-21 for H.O.) from Dokkyo Medical University.

Conflicts of Interest:

The authors declare that they have no conflicts of interest.

Ethical approval:

All applicable international, national, and/or institutional guidelines for the care and use of animals were followed. All procedures performed in studies involving animals were in accordance with the ethical standards of the institution or practice at which the studies were conducted.

REFERENCES

1. Björklund A, Dunnett SB (2007) Dopamine neuron systems in the brain: an update. Trends Neurosci 30 (5):194-202.
2. Skagerberg G, Lindvall O (1985) Organization of diencephalic dopamine neurons projecting to the spinal cord in the rat. Brain Res 342 (2):340-351.
3. Thorpe AJ, Clair A, Hochman S, Clemens S (2011) Possible sites of therapeutic action in restless legs syndrome: focus on dopamine and α2δ ligands. Eur Neurol 66 (1):18-29.
4. Charbit AR, Akerman S, Holland PR, Goadsby PJ (2009) Neurons of the dopaminergic/calcitonin gene-related peptide A11 cell group modulate neuronal firing in the trigeminocervical complex: an electrophysiological and immunohistochemical study. J Neurosci 29 (40):12532-12541.
5. Koblinger K, Füzesi T, Ejdrygiewicz J, Krajacic A, Bains JS, Whelan PJ (2014) Characterization of A11 neurons projecting to the spinal cord of mice. PLoS One 9 (10):e109636.
6. van den Pol AN (1986) Tyrosine hydroxylase immunoreactive neurons throughout the hypothalamus receive glutamate decarboxylase immunoreactive synapses: a double pre-embedding immunocytochemical study with particulate silver and HRP. J Neurosci 6 (3):877-891.
7. Pappas SS, Tiernan CT, Behrouz B, Jordan CL, Breedlove SM, Goudreau JL, et al (2010) Neonatal androgen-dependent sex differences in lumbar spinal cord dopamine concentrations and the number of A11 diencephalospinal dopamine neurons. J Comp Neurol 518 (13):2423-2436.
8. Abdallah K, Monconduit L, Artola A, Luccarini P, Dallel R (2015) GABAAergic inhibition or dopamine denervation of the A11 hypothalamic nucleus induces trigeminal analgesia. Pain 156 (4):644-655.
9. Rogers JH (1992) Immunohistochemical markers in rat brain: colocalization of calretinin and calbindin-D28k with tyrosine hydroxylase. Brain Res 587 (2):203-210.
10. González-Hernández T, Rodríguez M (2000) Compartmental organization and chemical profile of dopaminergic and GABAergic neurons in the substantia nigra of the rat. J Comp Neurol 421 (1):107-135.
11. Olson VG, Nestler EJ (2007) Topographical organization of GABAergic neurons within the ventral tegmental area of the rat. Synapse 61 (2):87-95.
12. Arai R, Jacobowitz DM, Deura S (1994) Distribution of calretinin, calbindin-D28k, and parvalbumin in the rat thalamus. Brain Res Bull 33 (5):595-614.
13. Gerfen CR, Baimbridge KG, Thibault J (1987) The neostriatal mosaic: III. Biochemical and developmental dissociation of patch-matrix mesostriatal systems. J Neurosci 7 (12):3935-3944.
14. Gerfen CR, Herkenham M, Thibault J (1987) The neostriatal mosaic: II. Patch- and matrix-directed mesostriatal dopaminergic and non-dopaminergic systems. J Neurosci 7 (12):3915-3934.
15. Celio MR (1990) Calbindin D-28k and parvalbumin in the rat nervous system. Neuroscience 35 (2):375-475.

16. Paxinos G, Watson C (2007) The rat brain in stereotaxic coordinates. Academic Press/Elsevier, Boston.
17. Carr DB, Sesack SR (2000) GABA-containing neurons in the rat ventral tegmental area project to the prefrontal cortex. Synapse 38 (2):114-123.
18. Gorelova N, Mulholland PJ, Chandler LJ, Seamans JK (2012) The glutamatergic component of the mesocortical pathway emanating from different subregions of the ventral midbrain. Cereb Cortex 22 (2):327-336.
19. Kawano M, Kawasaki A, Sakata-Haga H, Fukui Y, Kawano H, Nogami H et al (2006) Particular subpopulations of midbrain and hypothalamic dopamine neurons express vesicular glutamate transporter 2 in the rat brain. J Comp Neurol 498 (5):581-592.
20. Li X, Qi J, Yamaguchi T, Wang HL, Morales M (2013) Heterogeneous composition of dopamine neurons of the rat A10 region: molecular evidence for diverse signaling properties. Brain Struct Funct 218 (5):1159-1176.
21. Nair-Roberts RG, Chatelain-Badie SD, Benson E, White-Cooper H, Bolam JP, Ungless MA (2008) Stereological estimates of dopaminergic, GABAergic and glutamatergic neurons in the ventral tegmental area, substantia nigra and retrorubral field in the rat. Neuroscience 152 (4):1024-1031.
22. Tsumori T, Qin Y, Yokota S, Niu JG, Yasui Y (2010) Central amygdaloid axon terminals are in contact with retrorubral field neurons that project to the parvicellular reticular formation of the medulla oblongata in the rat. Brain Res 1306:18-28.
23. Yamaguchi T, Sheen W, Morales M (2007) Glutamatergic neurons are present in the rat ventral tegmental area. Eur J Neurosci 25 (1):106-118.
24. Yamaguchi T, Wang HL, Li X, Ng TH, Morales M (2011) Mesocorticolimbic glutamatergic pathway. J Neurosci; 31 (23):8476-8490.
25. Yamaguchi T, Wang HL, Morales M (2013) Glutamate neurons in the substantia nigra compacta and retrorubral field. Eur J Neurosci 38 (11):3602-3610.
26. Yamaguchi T, Qi J, Wang HL, Zhang S, Morales M (2015) Glutamatergic and dopaminergic neurons in the mouse ventral tegmental area. Eur J Neurosci 41 (6):760-772.
27. Neuhoff H, Neu A, Liss B, Roeper J (2002) I(h) channels contribute to the different functional properties of identified dopaminergic subpopulations in the midbrain. J Neurosci 22 (4):1290-1302.
28. Wang HL, Morales M (2009) Pedunculopontine and laterodorsal tegmental nuclei contain distinct populations of cholinergic, glutamatergic and GABAergic neurons in the rat. Eur J Neurosci 29 (2):340-358.
29. Martinez-Gonzalez C, Wang HL, Micklem BR, Bolam JP, Mena-Segovia J (2012) Subpopulations of cholinergic, GABAergic and glutamatergic neurons in the pedunculopontine nucleus contain calcium-binding proteins and are heterogeneously distributed. Eur J Neurosci 35 (5):723-734.
30. Frassoni C, Spreafico R, Bentivoglio M (1997) Glutamate, aspartate and co-localization with

calbindin in the medial thalamus. An immunohistochemical study in the rat. Exp Brain Res 115 (1):95-104.

31. Hu H, Gan J, Jonas P (2014) Interneurons. Fast-spiking, parvalbumin^{+} GABAergic interneurons: from cellular design to microcircuit function. Science 345 (6196):1255263.
32. Kosaka T, Kosaka K, Hataguchi Y, Nagatsu I, Wu JY, Ottersen OP et al (1987) Catecholaminergic neurons containing GABA-like and/or glutamic acid decarboxylase-like immunoreactivities in various brain regions of the rat. Exp Brain Res 66 (1):191-210.
33. Moriizumi T, Hattori T (1992) Anatomical and functional compartmentalization of the subparafascicular thalamic nucleus in the rat. Exp Brain Res 90 (1):175-179.
34. Pappas SS, Kennedy T, Goudreau JL, Lookingland KJ (2011) Opioid-mediated regulation of A11 diencephalospinal dopamine neurons: pharmacological evidence of activation by morphine. Neuropharmacol 61 (4):614-621.

FIGURE CAPTIONS

Fig. 1 Calbindin-immunoreactive (Calb-IR) cells were present throughout the entire A11 region with a gradient of distribution.

Sixteen-micrometer-thick rat brain coronal sections were processed for double immunofluorescent labeling for TH and Calb. Photomicrographs were taken under a fluorescence microscope for TH (red in a–c) and Calb (green in a'–c') at three levels (rostral, −3.16 mm; middle, −4.16 mm; caudal, −4.52 mm from bregma). Note that Calb-IR cells are intermingled with TH-IR cells throughout the entire A11 region, which is defined by the presence of large A11 TH neurons (arrows) distinguishable from small non-A11 TH neurons (arrowheads in c). Calb-IR neurons exhibit a gradient of distribution with a higher density at the middle of the A11 region (b'). 3V, third ventricle; fr, fornix retroflexus; mt, mammillothalamic tract. Scale bar in c' = 0.1 mm

Fig. 2 Three types of neurons with distinct neurochemical properties are present in the A11 region. Rat brain coronal sections, 16-µm-thick, were processed for double immunofluorescent labeling of TH and Calb. Lower magnification images were taken under a fluorescent microscope at three different levels from bregma (top panel; rostral, −3.16 mm; middle, −4.16 mm; caudal, −4.52 mm from bregma). Delimited areas in lower magnification pictures are shown at higher magnification under a fluorescence microscope, revealing TH (red in a–c) and Calb (green in a'–c') expression at the three levels. Merged pictures at each bregma level are also shown in a"– c". Note that the three cell types are intermingled in the A11 region; neurons co-expressing both TH and Calb (double arrows), neurons expressing TH, but not Calb (arrows), and neurons expressing Calb but not TH. Calb-IR processes extend among TH-IR cells. Calb-IR processes are also found close to TH-IR cells. 3V, third ventricle; A11, A11 region; fr, fornix retroflexus; mt, mammillothalamic tract. Scale bar in c' = 0.1 mm

Fig. 3 Schematic diagram of three neuron types observed in the A11 region.

Green, red, and blue dots represent Calb-, TH-, and Calb-/TH-double immunoreactive cell bodies, respectively. The average numbers of Calb-IR cell bodies observed at the three levels are shown in the left column, and the average numbers of TH- and TH-/Calb-double immunoreactive cell bodies are shown in the right column. 3V, third ventricle; fr, fornix retroflexus. rostral A11 region, −3.16 mm; middle, −4.16 mm; caudal, −4.52 mm from bregma.

Fig. 4 Parvalbumin-immunoreactive (PV-IR) processes were observed in the A11 region, but there were no PV-IR cell bodies. Sixteen-micrometer-thick rat brain coronal sections were processed for double immunofluorescent labeling for TH and GAD. Consecutive sections were processed for PV immunolabeling. Low magnification pictures taken under a fluorescence microscope show TH immunoreactivity (red in a–c) and GAD immunoreactivity (green in a"–c") at three levels (rostral, −3.16

mm; middle, −4.16 mm; caudal, −4.52 mm from bregma). Note that a large number of intensely GAD-IR processes were observed in the hypothalamus (ventral) region including A11, and more weakly GAD-IR processes were present in the thalamus (dorsal). The delimited areas in a–c are shown at higher magnification in d–f and areas corresponding to d–f in consecutive sections of Calb immunolabeling are shown in d'–f'. Arrows in d–f' indicate the locations of TH neurons. Note that PV-IR processes are found at the surrounding location where TH positive cells are present. 3V, third ventricle; fr, fasciculus retroflexus; mt, mammillothalamic tract. Scale bars = 0.1 mm (in c' for a – c'; in f' for d – f')

Fig. 5 Four types of A11 neurons were labeled by the retrograde tracer Fluorogold injected into the rat spinal cord. Rat brain coronal sections, 16-µm-thick, were prepared from brains of rats injected with Fluorogold (FG) into the spinal cord. The brain sections were processed for double immunofluorescent labeling of TH and Calb. Low-magnification images (a–a") were taken under a fluorescence microscope, revealing FG (blue in a), TH (red in a'), and Calb (green in a") expression. The delimited areas in a–a" are shown at higher magnification in b–d". Pictures in bb'–dd' are merged images of FG and TH immunolabeling, and bb"–dd" are merged images of FG and Calb immunolabeling. Note that four types of FG-positive neurons are observed in the A11 region: FG-positive neurons expressing both TH and Calb (double arrows), FG-positive neurons expressing TH and lacking Calb (arrows), FG-positive neurons lacking TH and expressing Calb (arrowheads), and FG-positive neurons lacking both TH and Calb (double arrowheads). TH-positive neurons lacking FG and Calb (open triangles) are also observed in d–d'. 3V, third ventricle; fr, fasciculus retroflexus. Scale bars = 0.1 mm (in a" for a–a" and in d" for b–d")

Figure 1

Click here to download Figure Fig 1 (TH-IR Calb-IR).tif

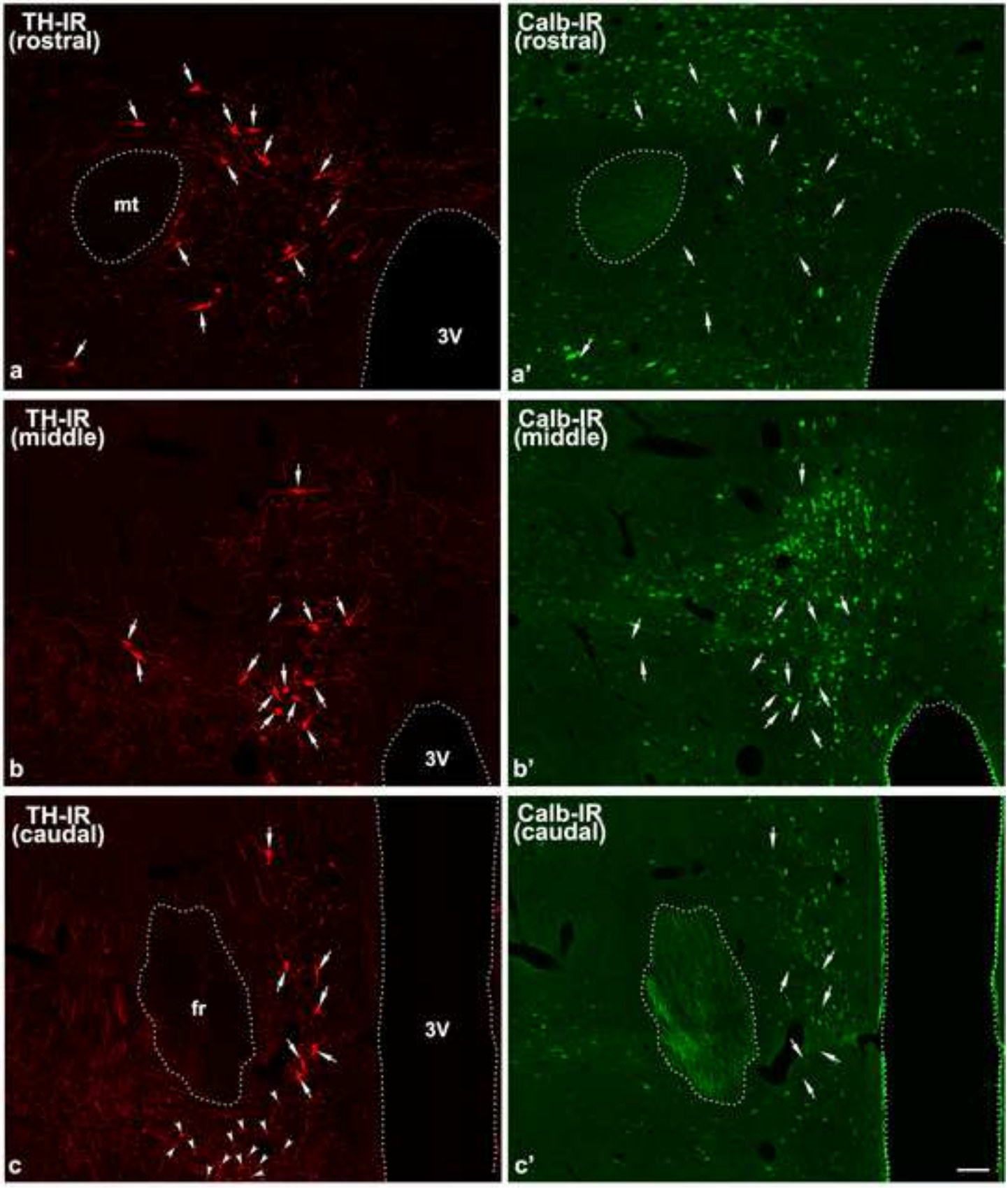

Figure 2

Click here to download Figure Fig 2 (TH-IR Calb-IR High Mag).tif

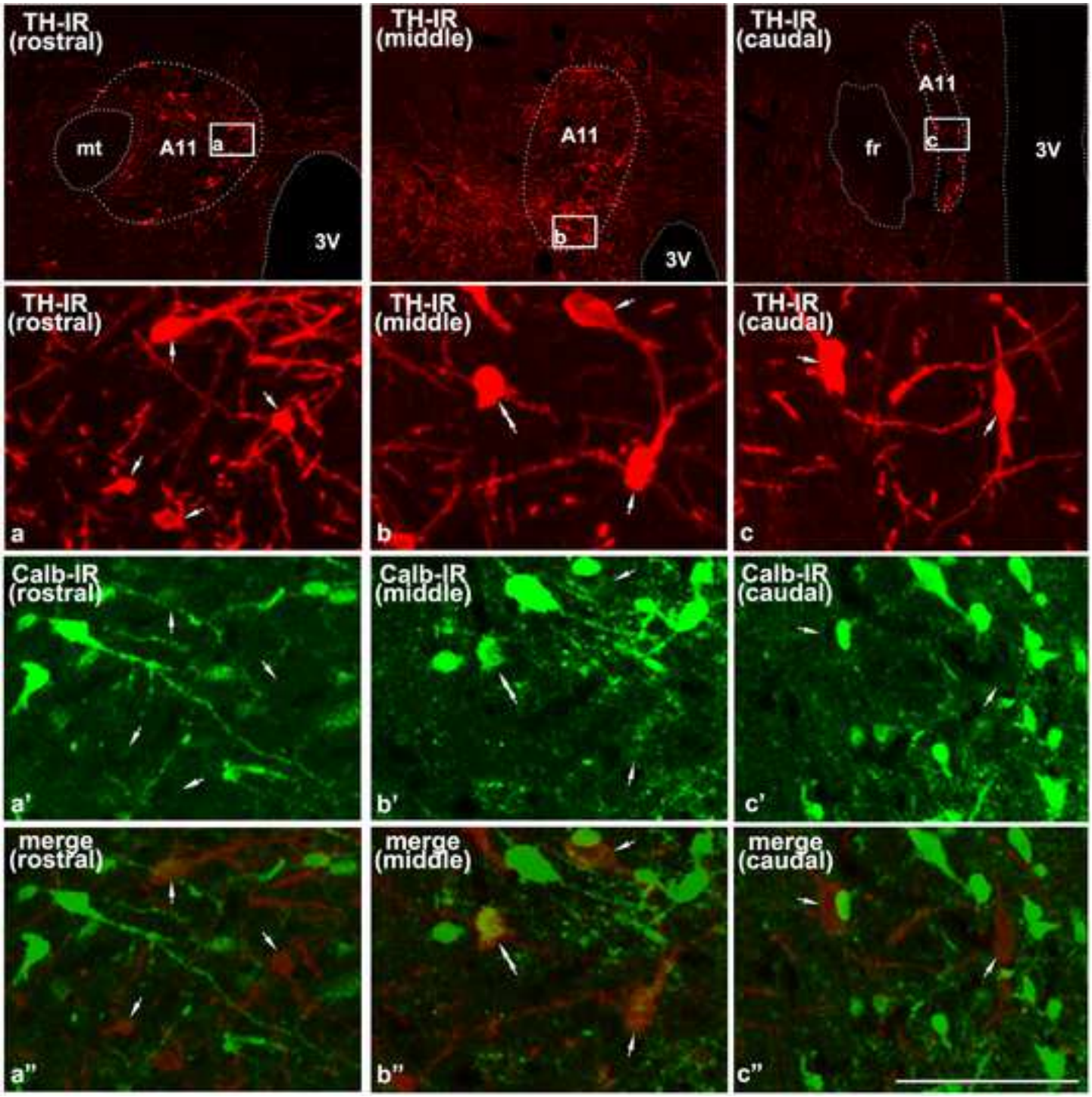

Figure 3

Click here to download Figure Fig 3 Diagram.tif

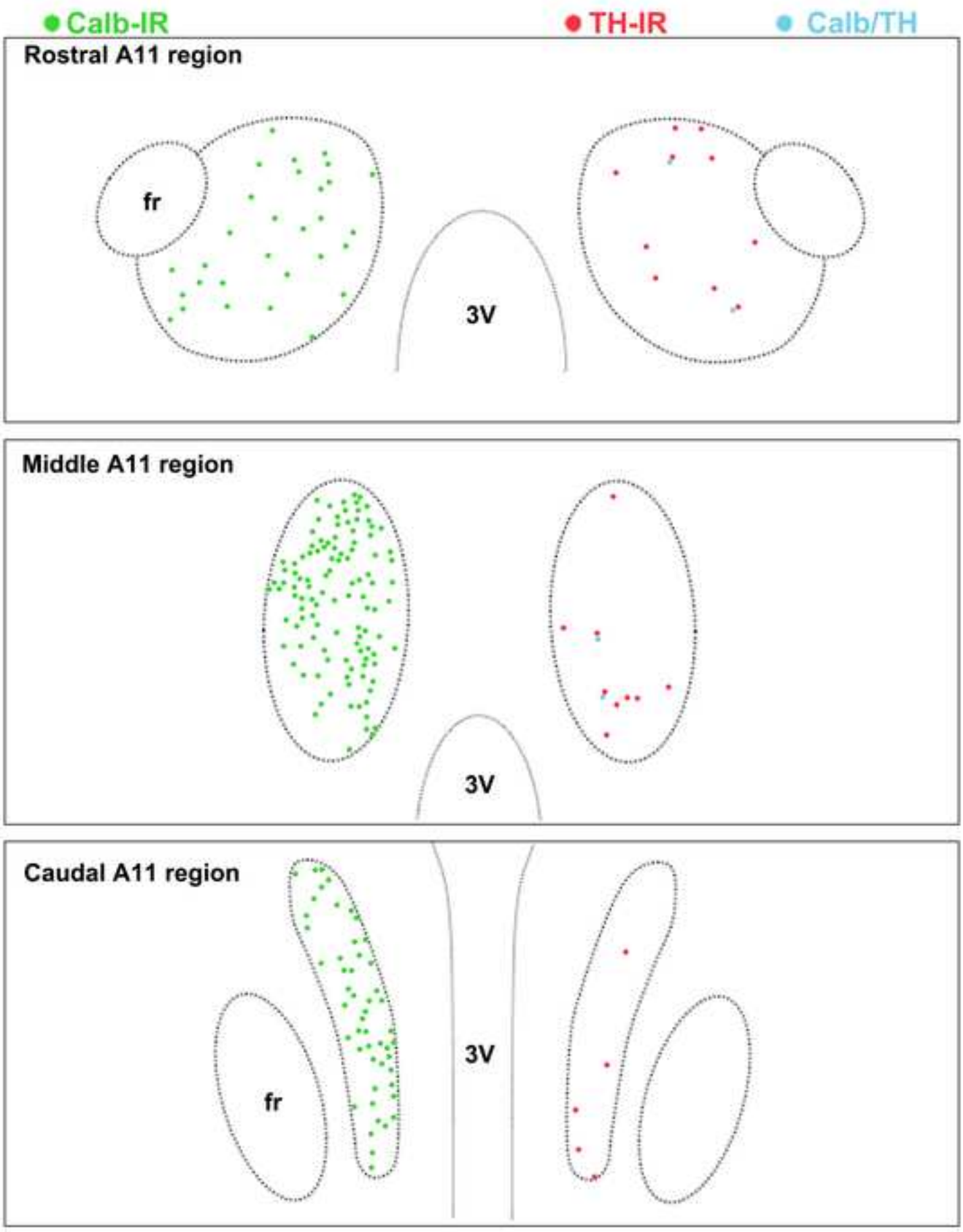

Figure 4

Click here to download Figure Fig 4 (TH-IR PV-IR High Mag).tif

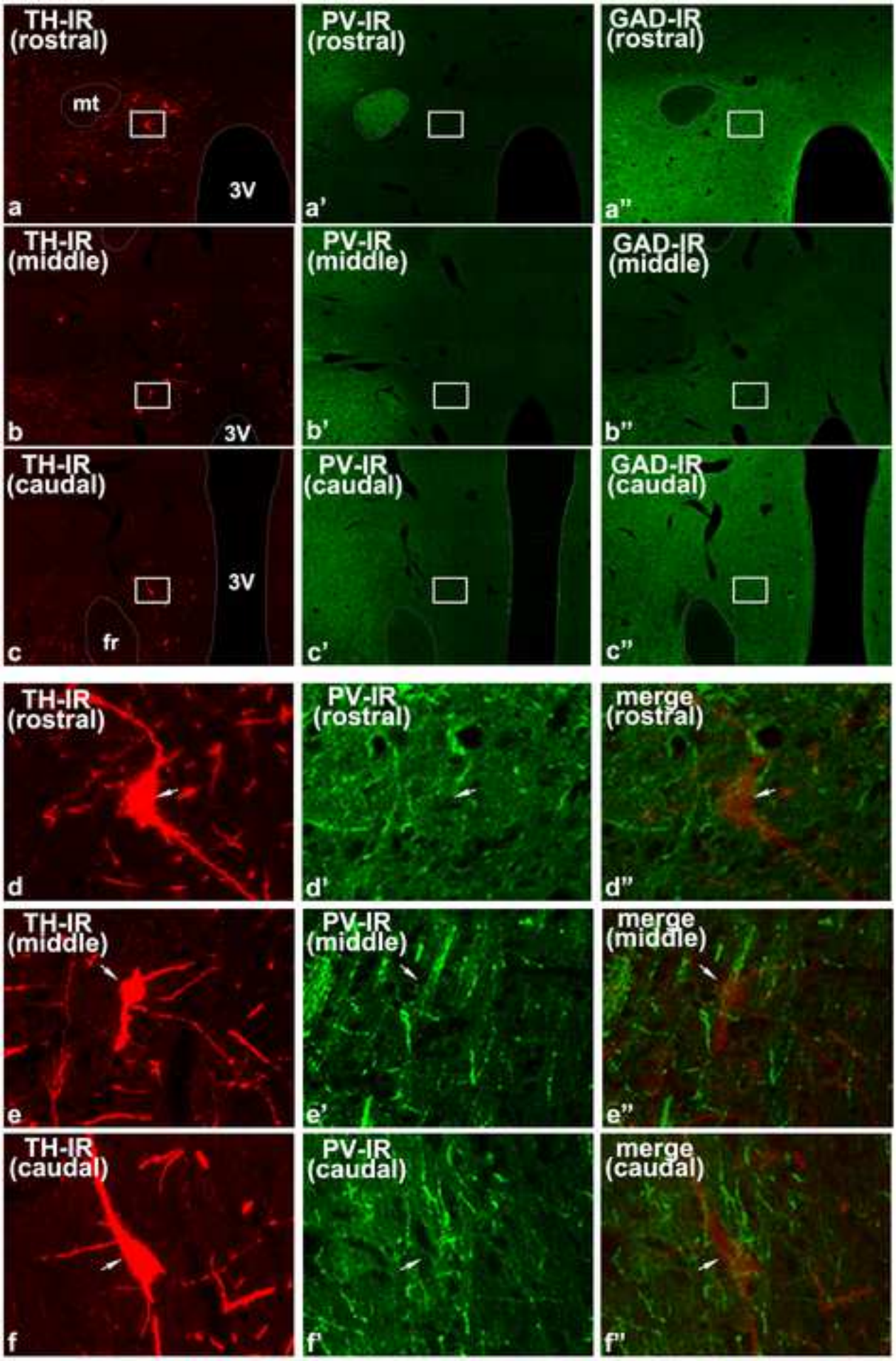

Figure 5

Click here to download Figure Fig5 (TH-IR Calb-IR FG).tif

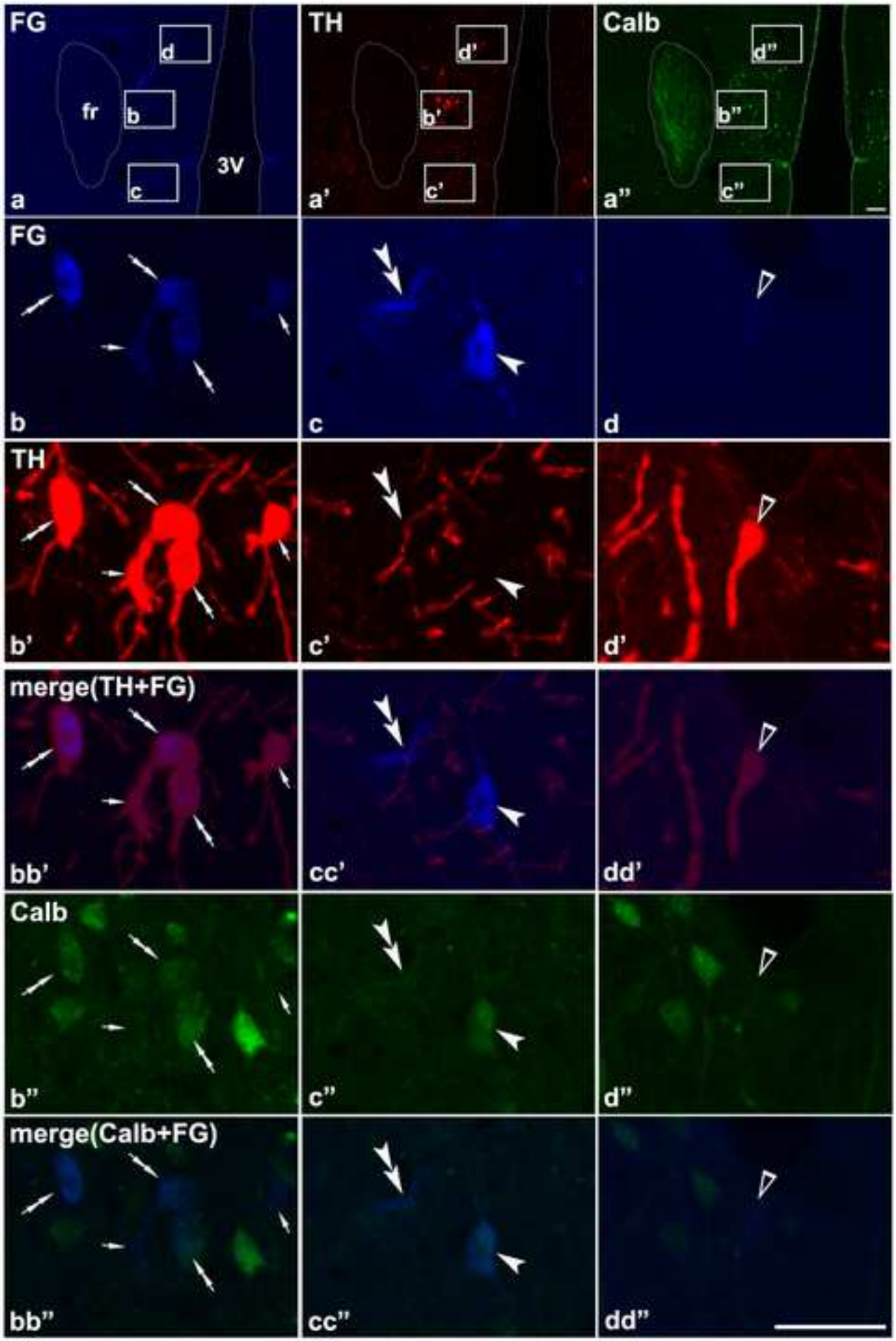

Quantification of three neuron types within the A11 region at three different levels

	Number of each type of neuron (mean ± SEM)			Percentage of Calb/TH in Calb or TH neurons	
	Calb	TH	Calb/TH	Calb/TH in Calb	Calb/TH in TH
rostral	35 ± 11	10 ± 1	2 ± 1	5.8 %	20.0%
middle	113 ± 15	9 ± 2	3 ± 1	2.5%	30.1%
caudal	51 ± 2	5 ± 1	0 ± 1	0.6%	6.3%

Each type of neuron (Calb, calbindin-immunoreactive; TH, tyrosine hydroxylase-immunoreactive; Calb/TH, Calbindin/TH-double positive) within the A11 region were quantified at three different levels (n = 4). The percentage of Calb/TH-double positive neurons in the total number of Calb or TH numbers were calculated for each subject.